

## Covalent Attachment of a Rhenium CO<sub>2</sub>-Reduction Catalyst to Rutile TiO<sub>2</sub>

Chantelle L. Anfuso<sup>(1)</sup>, Robert C. Snoeberger III<sup>(2)</sup>, Allen M. Ricks<sup>(1)</sup>, Weimin Liu<sup>(1)</sup>, Dequan Xiao<sup>(2)</sup>,

Victor S. Batista<sup>(2)\*</sup> and Tianquan Lian<sup>(1)\*</sup>

<sup>(1)</sup> Department of Chemistry, Emory University, Atlanta, GA 30322, U.S.A.; and

<sup>(2)</sup> Department of Chemistry, Yale University, New Haven, CT 06520-8107, U.S.A.

### Supporting Information

#### Sample Preparation.

Rutile (001) crystals were purchased from Commercial Crystal Laboratories, Inc. Prior to initial use, the crystals were sonicated in piranha solution (3:1 H<sub>2</sub>SO<sub>4</sub>/H<sub>2</sub>O<sub>2</sub>) for one hour, followed by a MilliQ (18 MΩ) water rinse. They were then placed in 1 M NaOH solution for 5 minutes, followed by another MilliQ rinse. The crystals were then placed in 1 M HCl solution and exposed to UV radiation for 10 minutes. After the UV treatment, the crystals were rinsed with ethanol and immediately immersed in a ReC0A/ethanol solution. The TiO<sub>2</sub> crystals were typically sensitized overnight, and then washed with ethanol to remove any nonadsorbed dye remaining on the TiO<sub>2</sub> surface prior to use. After preparation, the samples were stored in a dark, dry environment in order to preserve sample integrity for as long as possible. Between experiments, the crystals were cleaned by immersion in 1 M HCl for 5 minutes followed by immersion in 0.2 M NaOH for 5 minutes. This process was repeated a total of three times, rinsing the crystal with MilliQ water between each immersion. After cleaning, the previously outlined procedure for UV irradiation and sensitization was followed.

#### SFG experimental details

The SFG measurements were carried out using a 1 kHz Spitfire Ti:Sapphire regenerative amplifier system (Spectra Physics) producing 150 fs pulses at 800 nm with a pulse energy of 4 mJ. Half of the fundamental was used to pump a TOPAS-C OPA (Light Conversion) producing tunable IR pulses with energies of 10 – 20 μJ and a bandwidth of ~200 cm<sup>-1</sup>. The remaining 2 mJ of 800 nm was used to pump an SHBC/TOPAS-400 OPA (Light Conversion) system, producing tunable picosecond visible pulses from 480 – 800 nm with typical pulse energies of >50 μJ and a bandwidth of ~10 cm<sup>-1</sup>. The visible pulses were filtered to 2 – 10 μJ and combined with the IR at the sample. For the doubly-resonant study, the visible pulse power was held at 2 μJ for all wavelengths. The reflected sum frequency signal was collimated and filtered to remove any residual IR and fundamental visible photons before being refocused onto the slit of an imaging spectrograph (Acton Instruments SpectraPro 300i, 1200 groove/mm grating) and detected with an air-cooled CCD camera (Princeton Instruments VersArray 512B, 512 x 512 pixels) operating at -40.0°C. The polarization of the IR, visible, and SFG beams were controlled with polarizer/half-waveplate combinations. Nonresonant SFG spectra from gold were obtained previous to collecting data for ReC0A/TiO<sub>2</sub> (001) and used to normalize the ReC0A spectra.

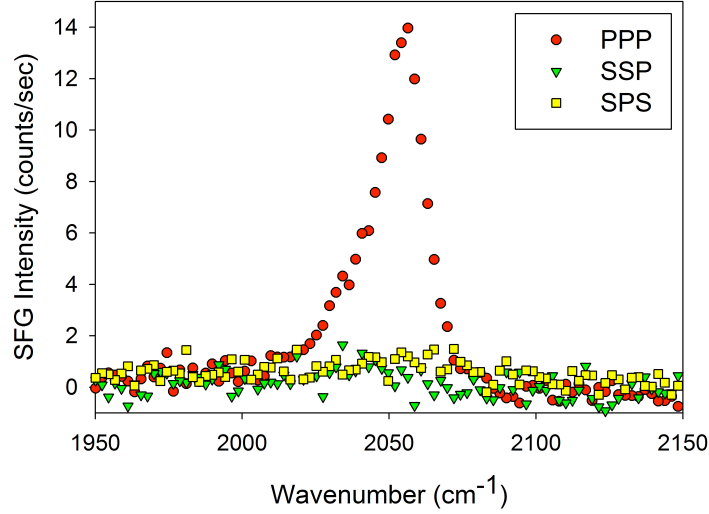


**Figure S1.** SFG spectra of ReCOA on TiO<sub>2</sub> (001) as a function of  $\omega_{\text{IR}}$  with  $\lambda_{\text{SF}} = 500$  nm for three polarization combinations: PPP (red circles), SSP (green triangles), and SPS (yellow squares).

### Sum Frequency Analysis

The theory of sum frequency generation has been examined in detail elsewhere and thus will be only briefly outlined here.<sup>1-5</sup> The intensity of the sum frequency signal is given by Equation (1) in the main text. The effective nonlinear susceptibility  $\chi_{\text{eff}}^{(2)}$  is related to individual susceptibility elements  $\chi_{ijk}^{(2)}$  ( $i, j, k = x, y, z$ ) by:

$$\chi_{\text{eff}}^{(2)} = [\hat{\mathbf{e}}(\omega) \cdot \mathbf{L}(\omega)] \cdot \chi^{(2)} : [\mathbf{L}(\omega_1) \cdot \hat{\mathbf{e}}(\omega_1)] [\mathbf{L}(\omega_2) \cdot \hat{\mathbf{e}}(\omega_2)] \quad (\text{S1})$$

where  $\hat{\mathbf{e}}(\Omega)$  is the unit polarization vector and  $\mathbf{L}(\Omega)$  is the Fresnel factor at frequency  $\Omega$ . Although there are 27  $\chi^{(2)}$  elements, for a molecule containing a mirror plane on a surface with C<sub>4</sub> symmetry – as in the case of ReCOA/TiO<sub>2</sub> (001) – only four independent nonzero  $\chi_{ijk}^{(2)}$  elements remain:  $\chi_{zzz}$ ,  $\chi_{xxz} = \chi_{yyz}$ ,  $\chi_{zxx} = \chi_{zyy}$ ,  $\chi_{zxy} = \chi_{zyx}$ , where z is the surface normal.<sup>6</sup> These independent components can be determined by measuring the sum-frequency signal using different input and output polarizations: SSP (S-polarized sum-frequency field, S-polarized visible field, and P-polarized infrared field), SPS, PSS, and PPP. The effective nonlinear susceptibilities for these polarization combinations are given by:<sup>4</sup>

$$\chi_{\text{eff,SSP}}^{(2)} = L_{yy}(\omega) L_{yy}(\omega_1) L_{zz}(\omega_2) \sin \beta_2 \chi_{yyz} \quad (\text{S2a})$$

$$\chi_{\text{eff,SPS}}^{(2)} = L_{yy}(\omega) L_{zz}(\omega_1) L_{yy}(\omega_2) \sin \beta_1 \chi_{zyy} \quad (\text{S2b})$$

$$\chi_{\text{eff,PSS}}^{(2)} = L_{zz}(\omega) L_{yy}(\omega_1) L_{yy}(\omega_2) \sin \beta \chi_{zyy} \quad (\text{S2c})$$

$$\begin{aligned} \chi_{\text{eff,PPP}}^{(2)} = & -L_{xx}(\omega) L_{xx}(\omega_1) L_{zz}(\omega_2) \cos \beta \cos \beta_1 \sin \beta_2 \chi_{xxz} \\ & - L_{xx}(\omega) L_{zz}(\omega_1) L_{xx}(\omega_2) \cos \beta \sin \beta_1 \cos \beta_2 \chi_{xxz} \\ & + L_{zz}(\omega) L_{xx}(\omega_1) L_{xx}(\omega_2) \sin \beta \cos \beta_1 \cos \beta_2 \chi_{zxx} \\ & + L_{zz}(\omega) L_{zz}(\omega_1) L_{zz}(\omega_2) \sin \beta \sin \beta_1 \sin \beta_2 \chi_{zzz} \end{aligned} \quad (\text{S2d})$$

where  $\beta$ 's are the incident angles of the denoted optical field and  $L_{ii}(\Omega)$  are Fresnel factors for frequency  $\Omega$ . These factors take into account the reflection, refraction, and enhancement of the fields due to the interface, and are typically of the form  $L_{ii}(\Omega)$ .<sup>2,4</sup>

$$L_{xx}(\Omega) = \frac{2n_1(\Omega) \cos \gamma}{n_1(\Omega) \cos \gamma + n_2(\Omega) \cos \beta} \quad (\text{S3a})$$

$$L_{yy}(\Omega) = \frac{2n_1(\Omega) \cos \beta}{n_1(\Omega) \cos \beta + n_2(\Omega) \cos \gamma} \quad (\text{S3b})$$

$$L_{zz}(\Omega) = \frac{2n_2(\Omega) \cos \beta}{n_1(\Omega) \cos \gamma + n_2(\Omega) \cos \beta} \left( \frac{n_1(\Omega)}{n'(\Omega)} \right) \quad (\text{S3c})$$

where  $n_i(\Omega)$  is the refractive index of medium  $i$ ,  $\beta$  is the incidence angle of the beam of interest,  $\gamma$  is the refracted angle, and  $n'(\Omega)$  the refractive index of the interfacial layer. This value is often taken as equal to  $n_1(\Omega)$ ,  $n_2(\Omega)$ , the average of the two, or the bulk refractive index of the material at the interface. A formalism was also detailed by Shen et al. in which  $n'(\Omega)$  is given by:<sup>4</sup>

$$\left( \frac{1}{n'} \right)^2 = \frac{4n_2^2 + 2}{n_2^2(n_2^2 + 5)} \quad (\text{S4})$$

For this work, we have elected to use Shen's expression, Eq. (5), to calculate  $n'(\Omega)$  values. We also explored using the other values of  $n'(\Omega)$  mentioned above to see how this affected the analysis. We found that changing the value of  $n'(\Omega)$  did not lead to radically different results, but did affect the range of orientation angles. For instance, choosing  $n'(\Omega) = n_{Air}$  led to a possible orientation angle of  $0 - 46^\circ$ , while choosing  $n'(\Omega) = n_{TiO_2}$  yielded a range of  $0 - 10^\circ$ . All of these results agree with the adsorption geometries predicted using DFT.

For a given molecule at an interface, the nonzero  $\chi^{(2)}_{ijk}$  elements are related to the second order hyperpolarizability elements  $\beta^{(2)}_{\alpha\beta\gamma}$  according to Equation (2) (see main text). In the case of SFG where the infrared frequency  $\omega_{IR}$  is in resonance with a molecular vibration, the second order hyperpolarizability elements are products of the infrared transition moment and the anti-Stokes Raman (AR) polarizability tensor:

$$\beta^{(2)}_{\alpha\beta\gamma}(-\omega_{sum}; \omega_{vis}, \omega_{IR}) = \beta^{(2)}_{NR} + \frac{-1}{2\hbar} \sum_n \frac{(\alpha_{0n}^{i'j'})_{AR} \mu_{n0}^{k'}}{(\omega_n - \omega_{IR} - i\Gamma_n)} \quad (\text{S5})$$

where  $\beta^{(2)}_{NR}$  is the nonresonant contribution due to material response (which is negligible for this study),  $\omega_n$  is the  $n^{\text{th}}$  resonant frequency and  $\Gamma_n$  is the damping constant of the  $n^{\text{th}}$  vibrational mode. Therefore, the SFG intensity is dependent on its IR and Raman cross sections. The nonzero hyperpolarizability elements for a particular molecule can often be determined by the molecular symmetry.<sup>4,7</sup> Assuming a dominant contribution of MLCT transition (along the c-axis) to the electronic resonance enhancement, two dominant hyperpolarizability elements are identified for the  $a'(1)$  modes:  $\beta_{ccc}$  and  $\beta_{ccb}$ , reflecting the fact that the transition dipole of the  $a'(1)$  mode lies in the c-b plane at an angle of  $28^\circ$  from the c-axis.<sup>8</sup>

Assuming these two hyperpolarizability elements, expressions for the relevant  $\chi^{(2)}$  elements can be written using Equation 2 (see main text). To determine the necessary  $\chi^{(2)}$  elements as a function of orientation angle  $\theta$ , we must average over the relevant  $\varphi$  and  $\psi$  angles. According to the calculated adsorption geometries, ReC0A may bind along any row of Ti atoms, as shown in Figures S2 and S3, so that the value of  $\varphi$  will always be  $(n\pi/4)$ , where  $n$  is an integer. The molecule binds to the surface with two functional groups and thus is not free to rotate, although the two configurations with the Cl atom along the b-axis or along the negative b-axis are equally likely, so that  $\psi = 0$  or  $\pi$ . Using these values of  $\varphi$  and  $\psi$ , we can generate the appropriate  $\chi^{(2)}$  elements as a function of the orientation angle and hyperpolarizability elements:

$$\chi_{zzz} = \cos^3(\theta) \cdot \beta_{ccc} \quad (\text{S6a})$$

$$\chi_{xxz} = \chi_{zxx} = \chi_{zzx} = \frac{1}{2} \cos(\theta) \sin^2(\theta) \cdot \beta_{ccb} \quad (\text{S6b})$$

As seen in Equation S6,  $\beta_{ccb}$  does not contribute to the  $\chi^{(2)}$  elements. These terms go to zero due to the assumption that the configurations with  $\psi = 0$  and  $\psi = \pi$  are equally likely. This is conceptually equivalent to imposing an a-c mirror plane for the molecule. In this case, according to symmetry arguments, all contributions with an odd number of  $b$  elements would go to zero.<sup>11</sup> Using these  $\chi^{(2)}$  elements, the relative PPP, SSP, and SPS intensities were simulated as a function of orientation angle using Equation S2, as seen in Figure 3 of the text.

## Computational Methods

DFT calculations were performed with the Vienna *Ab Initio* Simulation Package.<sup>9</sup> The PW91/GGA<sup>10</sup> density function was used to describe electron exchange and correlation. A plane-wave basis truncated with a 270 eV cutoff was used in all calculations as well as a single k-point sampling and ultrasoft Vanderbilt<sup>11</sup> pseudopotentials. The default convergence criteria were used for both the electronic energy and nuclear geometry optimizations.

The TiO<sub>2</sub> (001) surface was represented by a three-dimensional periodic slab with a vacuum in the [001] direction. The dimensions of the periodic surface were 1.38 by 0.92 nm<sup>2</sup> in the [010] and [100] directions, giving an adsorbate coverage of 0.79 adsorbate/nm<sup>2</sup>. The slab consisted of six layers of atoms, 0.73 nm thick. During the geometry relaxation of the ReC0A adsorbate, the TiO<sub>2</sub> atoms were held fixed at their crystal structure positions.<sup>12</sup>

Figure S2 shows a side, [010] direction, view (a) and a top-down, [001] direction, view (b) of the relaxed geometry of ReC0A adsorbed in the bidentate mode. It can be seen in the top-down view that the surface Ti atoms coordinated to the carboxylate groups are aligned in the [1-10] direction. The distance between the coordinated surface Ti atoms is 0.65 nm. The distance between carbon atoms of the carboxylate groups is 0.75 nm.

Figure S3 shows the relaxed geometry of ReC0A adsorbed in the tridentate mode, using the same views as Figure S2. It can be seen in the top-down view (a) that the surface Ti atoms coordinated to the carboxylate groups are aligned in the [010] direction. The distance between the surface Ti atoms in the [010] direction is 0.46 nm. The distance between carbon atoms of the carboxylate groups is 0.73 nm. The short distance between Ti atoms compared to the carboxylate distance favors the formation of the tridentate structure. Figure 3 (b) in the text gives a better view of this behavior.

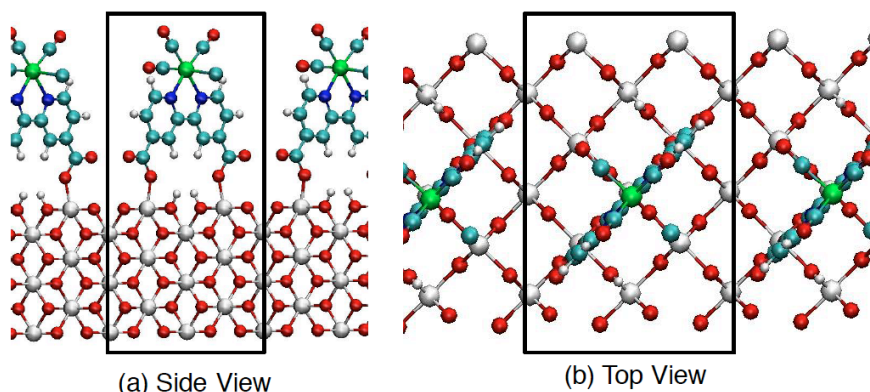


**Figure S2.** The (a) side view and the (b) top view of ReC0A adsorbed on the TiO<sub>2</sub> rutile (001) surface *via* the bidentate binding mode. The geometries were relaxed at the PW91/GGA level with the pseudopotential/plane wave approach and periodic boundary conditions. Color codes: H atoms (small white spheres), C atoms (cyan spheres), N atoms (blue spheres), O atoms (red spheres), Ti atoms (large white spheres), Cl atoms (large cyan spheres) and Re atoms (large green spheres).



- (9) Kresse, G.; Furthmüller, J. Efficient Iterative Schemes for Ab Initio Total-Energy Calculations Using a Plane-Wave Basis Set. *Physical Review B* **1996**, *54*, 11169-11186.
- (10) Perdew, J. P. In *Electronic Structure of Solids '91*; P. Ziesche, H. E., Ed.; Akademie Verlag: Berlin, 1991, p 11-20.
- (11) Vanderbilt, D. Soft Self-Consistent Pseudopotentials in a Generalized Eigenvalue Formalism. *Physical Review B* **1990**, *41*, 7892-7895.
- (12) Swope, R. J.; Smyth, J. R.; Larson, A. C. H in Rutile-Type Compounds .1. Single-Crystal Neutron and X-Ray-Diffraction Study of H in Rutile. *American Mineralogist* **1995**, *80*, 448-453.